

Phase-erased wavelength/format conversion and demodulation of 40 Gbit/s DPSK assisted by periodically poled lithium niobate

J. Wang · J. Sun · Q. Sun

Received: 19 March 2009 / Revised version: 9 November 2009 / Published online: 12 December 2009
© Springer-Verlag 2009

Abstract We report a novel phase-erased demodulation of differential phase-shift keying (DPSK) by exploiting cascaded second-harmonic generation and difference-frequency generation (cSHG/DFG) in a periodically poled lithium niobate (PPLN) waveguide. Analytical solutions are derived to clearly describe the operation principle. The binary optical phase information carried by the conventional DPSK demodulation outputs is removed thanks to the cSHG/DFG in a PPLN waveguide. PPLN-assisted phase-erased wavelength conversion and demodulation of 40 Gbit/s non-return-to-zero DPSK (NRZ-DPSK), return-to-zero DPSK (RZ-DPSK), and carrier-suppressed return-to-zero DPSK (CSRZ-DPSK) are demonstrated in the experiment. Moreover, the accompanying all-optical format conversions from optical duobinary (ODB) to NRZ and from ODB/alternate-mark inversion (AMI) to RZ are also substantiated in the experiment. In addition, the calculated theoretical results including optical spectra, temporal waveforms, and phase diagrams also confirm the successful implementation of PPLN-assisted 40 Gbit/s NRZ-DPSK/RZ-DPSK/CSRZ-DPSK phase-erased wavelength conversion, demodulation, and ODB-to-NRZ and ODB/AMI-to-RZ format conversions.

1 Introduction

In recent years, differential phase-shift keying (DPSK) has been emerging as an important advanced modulation format

for long-haul optical fiber transmission and high-speed optical communication systems owing to its high tolerance to chromatic dispersion and nonlinearity [1]. In DPSK modulation format the data information is encoded with binary optical phases of ‘0’ and ‘ π ’. A critical element in DPSK systems is regarded as the DPSK demodulator performing phase-to-intensity conversion prior to photodiode [1]. Previously, several attractive candidates and lots of schemes were employed to perform DPSK demodulation with impressive operation performance, including injection locking of a semiconductor laser diode [2], birefringent-fiber-loop [3], ultranarrow optical discriminator filter [4], athermal delay-interferometer filter [5–7], polarization Mach-Zehnder delay interferometer implemented with a highly birefringent air-guiding photonic bandgap (PBG) fiber [8], silicon-based microring resonator [9], fiber Bragg grating filters [10, 11], stimulated-Brillouin-scattering-based optical filtering [12], silicon-on-insulator delay interferometer [13], tunable differential group delay (DGD) element [14], delay-asymmetric nonlinear loop mirror [15]. These schemes demodulated the DPSK signal into an intensity-modulated signal for detection. However, it should be noted that the demodulation output using all the previous approaches had binary optical phase variation. For instance, the constructive demodulation output takes the optical duobinary (ODB) format while the destructive demodulation output carries the alternate-mark inversion (AMI) format [6, 9]. Both ODB and AMI contain binary optical phase variation with a relative phase difference of π . So far phase-removed DPSK demodulation has not yet been demonstrated.

Very recently, a promising candidate known as quasi-phase matched (QPM) periodically poled lithium niobate (PPLN) waveguide has been widely used for various high-speed all-optical signal processing applications for its distinct advantages of large nonlinear coefficient, ultrafast

J. Wang · J. Sun (✉) · Q. Sun

Wuhan National Laboratory for Optoelectronics, College of Optoelectronic Science and Engineering, Huazhong University of Science and Technology, Wuhan 430074, Hubei, China
e-mail: jqsun@mail.hust.edu.cn

Fax: +86-27-87792225

nonlinear optical response, negligible spontaneous emission noise, and miscellaneous second-order and cascaded second-order nonlinearities [16]. PPLN-based wavelength conversions [17–23], optical tunable delays [24–26], optical switching [27], label swapping [28], logic gates [29–33], format conversions [34], and optical phase conjugation for dispersion compensation [35] have been demonstrated. Previously, we have suggested and confirmed a new optical phase erasure characteristic of PPLN [36], based on which all-optical format conversion from carrier-suppressed return-to-zero (CSRZ) to return-to-zero (RZ) has been performed [36].

In this paper, by using the optical phase erasure characteristic of PPLN based on cascaded second-harmonic generation and difference-frequency generation (cSHG/DFG), we report another new application of PPLN in phase-erased demodulation of DPSK modulation format. We experimentally demonstrate phase-erased wavelength conversion and demodulation of 40 Gbit/s non-return-to-zero DPSK (NRZ-DPSK), RZ-DPSK, and CSRZ-DPSK assisted by removing the binary optical phase variation in the conventional demodulation outputs. Furthermore, all-optical format conversions at 40 Gbit/s from ODB to NRZ and from ODB/AMI to RZ are also implemented.

2 Experimental setup and operation principle

Figure 1 illustrates the conventional demodulation of 40 Gbit/s DPSK using a 40G fiber delay interferometer (FDI). It consists of two 3 dB optical couplers (OCs) and two fiber arms with a length difference of 5.2 mm, which introduces a relative time delay of 25 ps (Δt). The operation

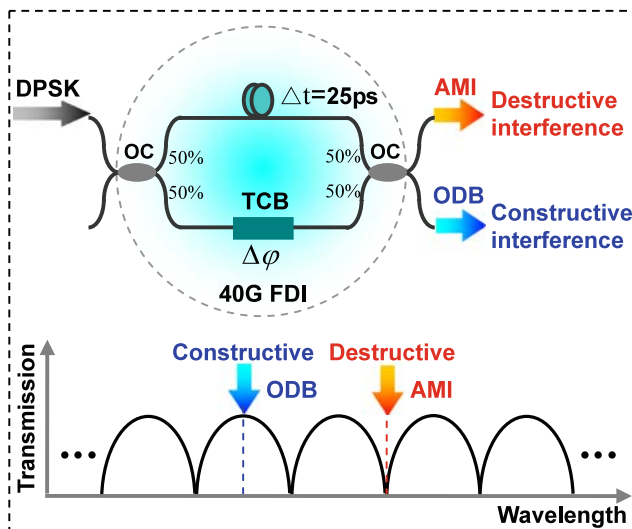


Fig. 1 Schematic illustration of conventional 40 Gbit/s DPSK demodulation using a 40G FDI

temperature of the lower arm is controlled by a temperature controlling block (TCB) to adjust the phase shift ($\Delta\varphi$). Such one-bit-delay 40G FDI can perform the conventional demodulation of 40 Gbit/s DPSK. It should be noted that the demodulation outputs from 40G FDI are not exactly the NRZ or RZ modulation format, which has constant optical phase. In general, it is ODB and AMI modulation formats that are respectively obtained at the constructive interference output port and destructive interference output port of 40G FDI. Remarkably, ODB/AMI modulation format has a similar power profile to that of NRZ/RZ. However, there also exists distinct difference between ODB/AMI and NRZ/RZ with the fact that ODB/AMI has binary optical phase variation in its data bits.

Figure 2 shows the experimental setup and operation principle for PPLN-assisted phase-erased DPSK demodulation. 40 Gbit/s pseudo-random binary sequence (PRBS)

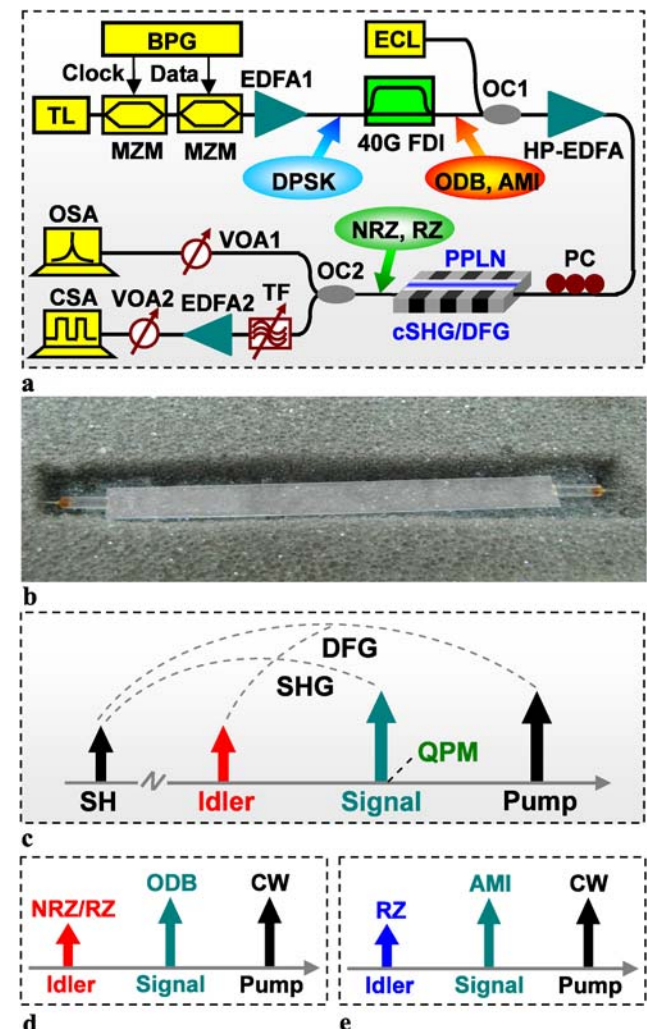


Fig. 2 (a) and (b) Experimental setup and (c)–(e) operation principle for PPLN-assisted phase-erased wavelength/format conversion and demodulation of 40 Gbit/s NRZ-DPSK/RZ-DPSK/CSRZ-DPSK. TF: tunable filter; VOA: variable optical attenuator

NRZ-DPSK/RZ-DPSK/CSRZ-DPSK signal is generated from a tunable laser (TL), two cascaded Mach-Zehnder modulators (MZMs) driven by a bit pattern generator (BPG), and an erbium-doped fiber amplifier (EDFA). A 40G FDI is employed to demodulate the 40 Gbit/s DPSK signal. Note that the direct demodulation outputs from 40G FDI take ODB (constructive interference) and AMI (destructive interference) modulation formats, which have binary optical phase variation with a relative phase difference of π . The demodulated ODB/AMI signal, together with a continuous-wave (CW) pump emitted from an external cavity laser (ECL), are combined by an optical coupler (OC), amplified by a high-power erbium-doped fiber amplifier (HP-EDFA), polarization state adjusted through a polarization controller (PC), and finally launched into PPLN to take part in the cSHG/DFG nonlinear interactions. The HP-EDFA offers a small-signal gain of 40 dB and a saturation output power of 30 dBm. Figure 2(b) depicts the photograph of the PPLN waveguide adopted in the experiment which is fabricated by the electric-field poling method and annealing proton-exchanged technique. It has a microdomain period of $14.7 \mu\text{m}$ and a QPM wavelength of $\sim 1543.2 \text{ nm}$ at room temperature during the experiment. The optical spectra and temporal waveforms are respectively observed via an optical spectrum analyzer (OSA, Anritsu MS9710C) with the highest spectral resolution of 0.05 nm and a communications signal analyzer (CSA, Tektronix 8000B).

For cSHG/DFG processes, as shown in Figs. 2(c)–(e), here the ODB/AMI signal not the CW pump is set at the SHG QPM wavelength of PPLN. The ODB/AMI signal is converted to a second-harmonic (SH) wave by SHG, which simultaneously interacts with the CW pump to yield a new converted idler wave by the subsequent DFG. We can derive an analytical solution to the complex amplitude of the converted idler (A_i) under non-depletion approximation expressed as

$$A_i = C \cdot A_S^2 A_P^* \quad (1)$$

$$C = -\frac{1}{2} \omega_i \omega_{\text{SH}} \kappa_{\text{SH}} \kappa_{\text{DFG}} \left\{ \left[\frac{L}{\Delta} \sin(\Delta L) + \frac{\cos(\Delta L) - 1}{\Delta^2} \right] + i \left[\frac{\sin(\Delta L)}{\Delta^2} - \frac{L}{\Delta} \cos(\Delta L) \right] \right\} \quad (2)$$

where C is a constant, A_S and A_P are respective complex amplitudes of input signal and pump. ω_i and ω_{SH} are angular frequencies of idler and SH wave. κ_{SH} and κ_{DFG} are coupling coefficients of SHG and DFG. Δ is phase mismatch of DFG. L is the length of PPLN. We can further deduce following complex amplitude (A) and optical phase (ϕ) relationships as

$$A_i \propto A_S^2 A_P^* \quad (3)$$

$$\phi_i \propto 2\phi_S - \phi_P \quad (4)$$

According to (1), (3) and (4) and taking into account the periodicity of 2π of optical phase, the square relationship between converted idler and input signal implies that the binary optical phase variation with a relative difference of π ($\phi_0, \phi_0 + \pi$) in the signal can be removed in the converted idler ($\phi_0 \rightarrow 2\phi_0, \phi_0 + \pi \rightarrow 2\phi_0 + 2\pi = 2\phi_0$). In addition, after removing the binary optical phase variation, ODB signal is converted to NRZ/RZ idler (Fig. 2(d)) and AMI signal is transformed to RZ idler (Fig. 2(e)). As a result, it is possible to perform PPLN-assisted phase-erased NRZ-DPSK/RZ-DPSK/CSRZ-DPSK demodulation and ODB-to-NRZ/RZ, AMI-to-RZ format conversions.

3 Experimental results and discussions

Phase-erased wavelength/format conversion and demodulation for 40 Gbit/s NRZ-DPSK, RZ-DPSK, CSRZ-DPSK signals are in turn performed. Figure 3 depicts the measured typical optical spectra for conventional 40 Gbit/s NRZ-DPSK demodulation using a 40G FDI. The constructive interference demodulation takes the ODB format as shown in Fig. 3(b) while the destructive interference demodulation with the carrier suppressed has the AMI format as shown in Fig. 3(c).

Figure 4 shows the measured optical spectra for PPLN-assisted phase-erased 40 Gbit/s NRZ-DPSK demodulation and ODB-to-NRZ format conversion. ODB signal is set at 1543.2 nm to meet the SHG QPM condition. The converted idler is generated at 1535.1 nm as the CW pump is tuned at 1551.4 nm . Insets (a) and (b) show the enlarged spectra for ODB signal and NRZ idler. It is found

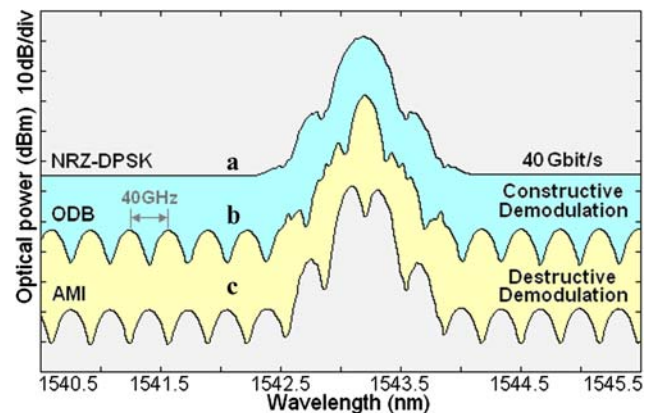


Fig. 3 Measured optical spectra for conventional 40 Gbit/s NRZ-DPSK demodulation using a 40G FDI. (a) Input NRZ-DPSK; (b) Constructive interference demodulation with ODB format; (c) Destructive interference demodulation with AMI format

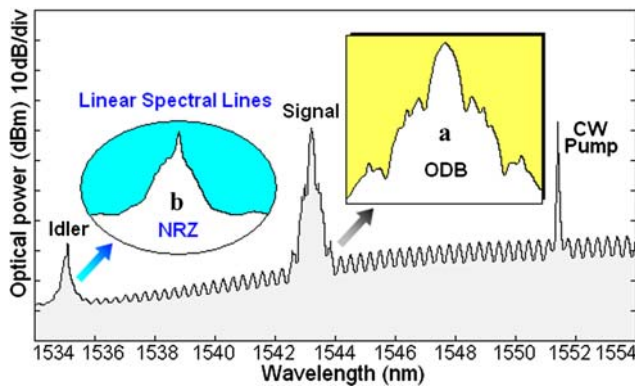


Fig. 4 Measured optical spectra for 40 Gbit/s NRZ-DPSK phase-erased demodulation and ODB-to-NRZ format conversion

that linear spectral line is present in the converted idler, which has the spectrum similar to NRZ modulation format. The spectral difference between the ODB signal and NRZ idler can be explained with the fact the binary optical phase information in the ODB signal is erased in the NRZ idler.

Figure 5 depicts the measured optical spectra for PPLN-assisted phase-erased 40 Gbit/s NRZ-DPSK demodulation and AMI-to-RZ format conversion. AMI signal is set at 1543.2 nm to satisfy the SHG QPM condition. The idler at 1535.1 nm is obtained with the CW pump set at 1551.4 nm. As can be clearly seen from the insets, the idler shown in inset (b) has a similar spectrum to RZ modulation format, which is quite different from the AMI signal shown in inset (a). The carrier is suppressed in AMI signal while present in RZ idler. We can observe clear linear spectral lines in the RZ idler. Such phenomenon can be attributed to optical phase erasure from AMI signal to RZ idler.

Figure 6 displays the observed temporal waveforms for different optical waves, from which we can clearly see that the intensity information carried by ODB/AMI is successfully copied onto converted NRZ/RZ idlers. Figures 4, 5 and 6 indicate the successful implementation of phase-erased 40 Gbit/s NRZ-DPSK demodulation and ODB-to-NRZ and AMI-to-RZ format conversions. Note that the optical phase information is not reflected in the waveforms. However, we can deduce the conclusion of optical phase removal from the change of optical spectra. The ODB/AMI signal has smooth spectra owing to the binary optical phase variation in the data bits. By contrast, after removing the binary optical phase information, the generated NRZ/RZ idler has shown clear linear spectral lines in the spectra.

To further confirm the proposed PPLN-assisted phase-erased NRZ-DPSK demodulation and ODB-to-NRZ and AMI-to-RZ format conversions, we also present the theoretical results according to (3) including optical spectra, temporal waveforms, and phase diagrams as shown

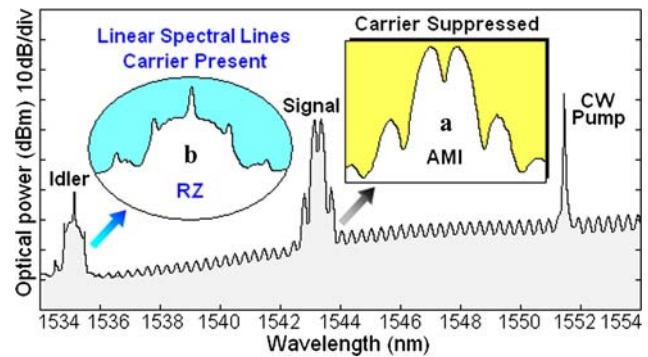


Fig. 5 Measured optical spectra for 40 Gbit/s NRZ-DPSK phase-erased demodulation and AMI-to-RZ format conversion

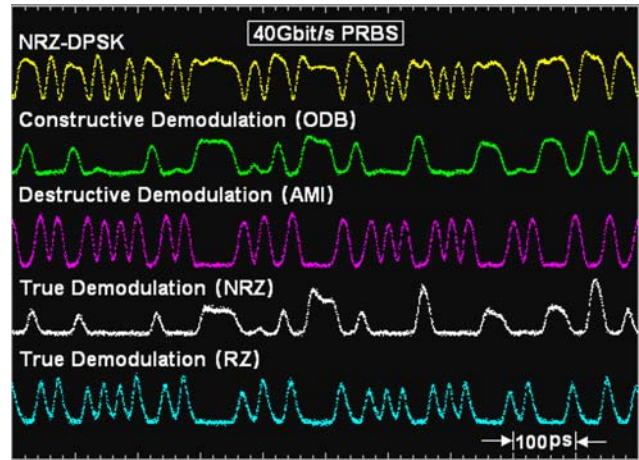
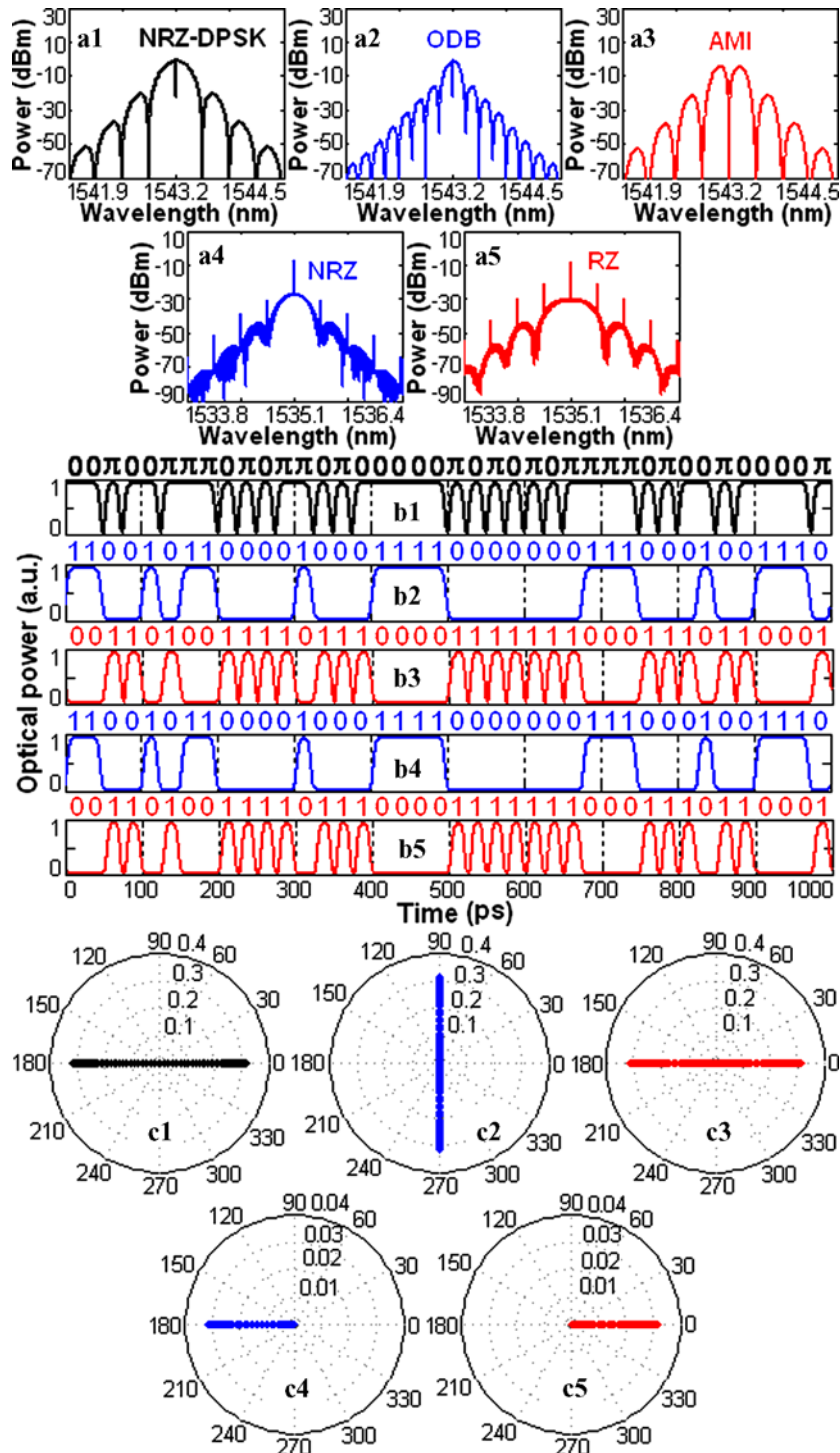


Fig. 6 Measured temporal waveforms for different optical waves corresponding to phase-erased 40 Gbit/s NRZ-DPSK demodulation

in Fig. 7. A 40 Gbit/s PRBS NRZ-DPSK signal is considered. As shown in Figs. 7(a2) and (a3), the conventional demodulated ODB/AMI signals have smooth spectra while the converted idlers by cSHG/DFG have linear spectral lines similar to NRZ/RZ modulation formats as depicted in Figs. 7(a4) and (a5). The obtained spectra and waveforms by theoretical analyses are in good agreement with the experimental results. We also plot phase diagrams for different optical waves. It can be clearly seen that ODB/AMI have binary phase variation with a relative phase difference of π as shown in Figs. 7(c2) and (c3). With the assistance of optical phase removal using cSHG/DFG in a PPLN waveguide, it is found that the converted RZ idlers have constant optical phase as depicted in Figs. 7(c4) and (c5). As a consequence, we can conclude from the experimental and theoretical results shown in Figs. 4, 5, 6 and 7 that PPLN-assisted phase-erased wavelength conversion and demodulation of 40 Gbit/s NRZ-DPSK and ODB-to-NRZ, AMI-to-RZ format conversion are successfully implemented.

Fig. 7 Theoretical results for phase-erased 40 Gbit/s NRZ-DPSK demodulation and ODB-to-NRZ, AMI-to-RZ format conversions.

(a1)–(a5) Optical spectra; (b1)–(b5) Temporal waveforms; (c1)–(c5) Phase diagrams; (a1), (b1) and (c1) NRZ-DPSK signal; (a2), (b2) and (c2) ODB signal; (a3), (b3) and (c3) AMI signal; (a4), (b4) and (c4) NRZ idler (ODB-to-NRZ); (a5), (b5) and (c5) RZ idler (AMI-to-RZ)



In addition to NRZ-DPSK, it is also possible to perform PPLN-assisted phase-erased wavelength/format conversion and demodulation for 40 Gbit/s RZ-DPSK and CSRZ-DPSK signals. Figures 8(a) and (b) show the spectra observed in the experiment when 40 Gbit/s RZ-DPSK is employed. The spectra of ODB and AMI directly demodulated from RZ-DPSK are smooth. However, linear spectral

lines with a spacing of 40 GHz are obtained in the converted idlers which take the RZ format. These changes in the spectra can be ascribed to the binary optical phase erasure from ODB/AMI to the converted RZ idlers. The theoretical results shown in Figs. 8(a1), (a2), (b1) and (b2) are consistent with those observed in the experiment. Very similar to Fig. 8, Fig. 9 depicts both experimentally observed and theoreti-

Fig. 8 Measured optical spectra for 40 Gbit/s RZ-DPSK phase-erased demodulation accompanied by (a) ODB-to-RZ and (b) AMI-to-RZ format conversions. (a1), (a2), (b1) and (b2) Theoretical results of optical spectra. (a1) ODB signal; (a2) RZ idler (ODB-to-RZ); (b1) AMI signal; (b2) RZ idler (AMI-to-RZ)

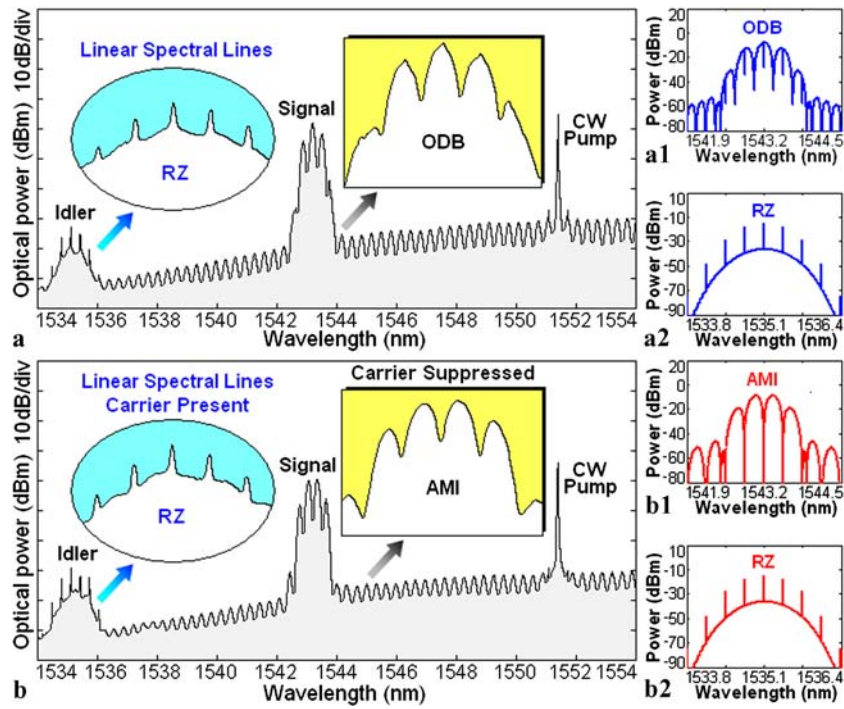
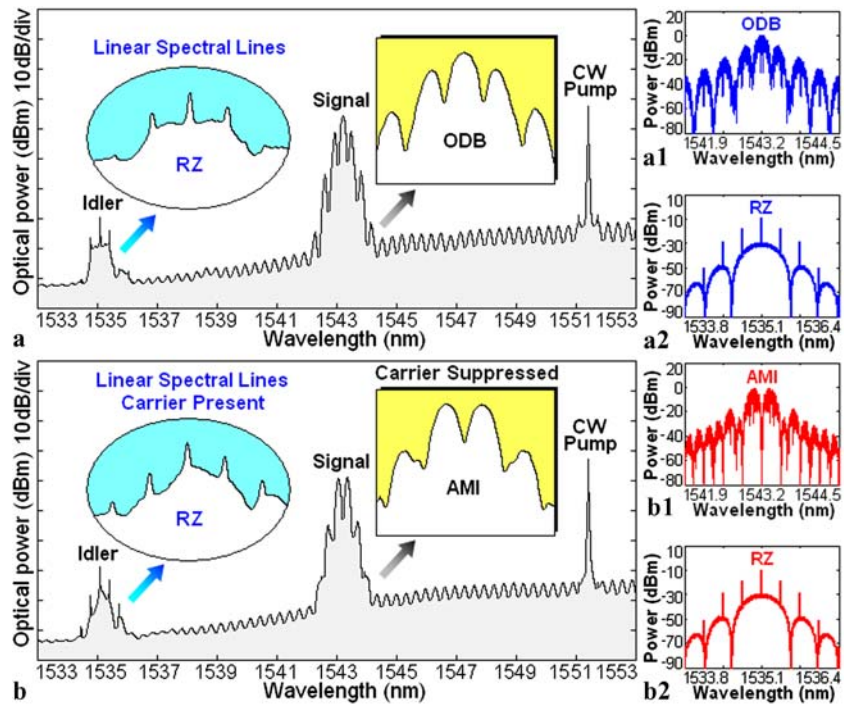


Fig. 9 Measured optical spectra for 40 Gbit/s CSRZ-DPSK phase-erased demodulation accompanied by (a) ODB-to-RZ and (b) AMI-to-RZ format conversions. (a1), (a2), (b1) and (b2) Theoretical results of optical spectra. (a1) ODB signal; (a2) RZ idler (ODB-to-RZ); (b1) AMI signal; (b2) RZ idler (AMI-to-RZ)



cally calculated spectra as 40 Gbit/s CSRZ-DPSK is considered. Besides the spectra, Figs. 10(a) and (b) further display the temporal waveforms observed in the experiment when 40 Gbit/s RZ-DPSK and CSRZ-DPSK are respectively adopted. Simple theoretical calculations of waveforms conform to the experiment results. The analogous theoretically calculated phase diagrams to those plotted in Figs. 7(c1)–

(c5) are not shown here for RZ-DPSK and CSRZ-DPSK. Compared to the case of NRZ-DPSK as shown in Figs. 3, 4, 5, 6 and 7, here the difference is that after optical phase removal the ODB is changed to the RZ format but not the NRZ format for the cases of RZ-DPSK and CSRZ-DPSK. As a result, phase-erased demodulation accompanied by all-optical ODB-to-NRZ, AMI-to-RZ format conversions are

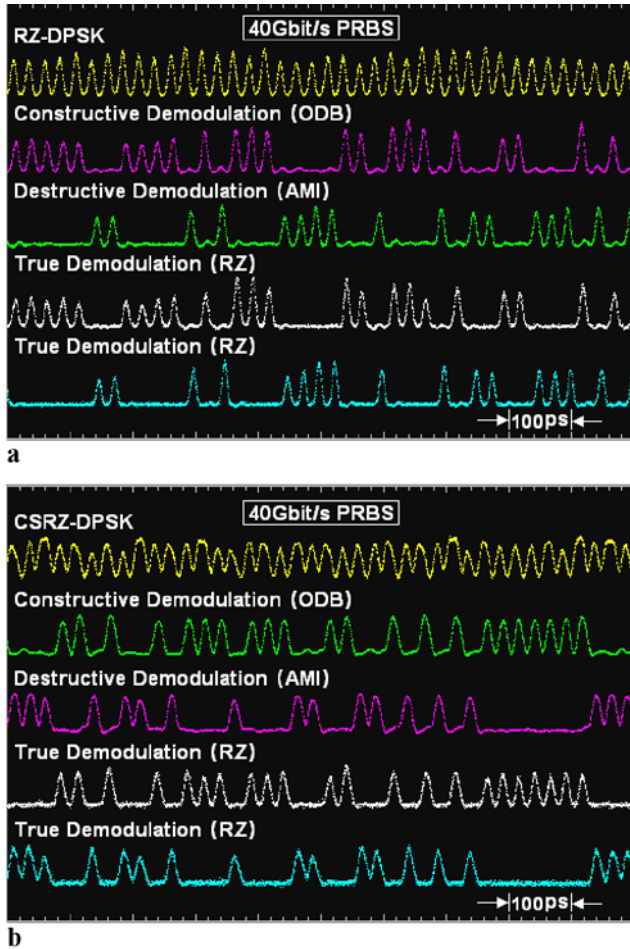


Fig. 10 Measured temporal waveforms for different optical waves corresponding to phase-erased 40 Gbit/s (a) RZ-DPSK and (b) CSRZ-DPSK demodulation

achieved when 40 Gbit/s NRZ-DPSK is employed. When 40 Gbit/s RZ-DPSK/CSRZ-DPSK is used, phase-erased demodulation together with all-optical ODB-to-RZ, AMI-to-RZ format conversions are implemented.

4 Conclusion

In summary, we propose and demonstrate phase-erased demodulation of 40 Gbit/s NRZ-DPSK/RZ-DPSK/CSRZ-DPSK signals based on cSHG/DFG in a PPLN waveguide. Moreover, with the assistance of optical phase erasure characteristic of PPLN, all-optical 40 Gbit/s ODB-to-NRZ/RZ and AMI-to-RZ format conversions are also implemented in the experiment. The obtained theoretical results including optical spectra, temporal waveforms, and phase diagrams further verify the successful implementation of PPLN-assisted phase-erased 40 Gbit/s NRZ-DPSK/RZ-DPSK/CSRZ-DPSK demodulation and ODB-to-NRZ/RZ and AMI-to-RZ format conversions.

Acknowledgements This work was supported by the Natural Science Foundation of Hubei Province of China under Grant No. 2008-CDB313 and National Natural Science Foundation of China under Grant No. 60577006. The authors would like to sincerely thank M.M. Fejer and J.R. Kurz at Stanford University for fabricating the PPLN waveguide used in the experiments.

References

1. P.J. Winzer, R.-J. Essiambre, *J. Lightwave Technol.* **24**, 4711 (2006)
2. Y. Awaji, T. Kuri, W. Chujo, *IEEE Photon. Technol. Lett.* **14**, 1007 (2002)
3. C.W. Chow, H.K. Tsang, *IEEE Photon. Technol. Lett.* **17**, 1313 (2005)
4. I. Lyubomirsky, C.C. Chien, *IEEE Photon. Technol. Lett.* **17**, 492 (2005)
5. X. Liu, A.H. Gnauck, X. Wei, J. Hsieh, C. Ai, V. Chien, *IEEE Photon. Technol. Lett.* **17**, 2610 (2005)
6. A.H. Gnauck, X. Liu, S. Chandrasekhar, X. Wei, *IEEE Photon. Technol. Lett.* **18**, 637 (2006)
7. Y.K. Lizé, M. Faucher, É. Jarry, P. Ouellette, É. Villeneuve, A. Wetter, F. Séguin, *IEEE Photon. Technol. Lett.* **19**, 1886 (2007)
8. C. Peucheret, Y. Geng, B. Zsigri, T.T. Alkeskjold, T.P. Hansen, P. Jeppesen, *IEEE Photon. Technol. Lett.* **18**, 1392 (2006)
9. L. Zhang, J.Y. Yang, M.P. Song, Y.C. Li, B. Zhang, R.G. Beausoleil, A.E. Willner, *Opt. Express* **15**, 11564 (2007)
10. T.-Y. Kim, M. Hanawa, S.-J. Kim, S. Hann, Y.H. Kim, W.-T. Han, C.-S. Park, *IEEE Photon. Technol. Lett.* **18**, 1834 (2006)
11. G. Contestabile, R. Proietti, N. Calabretta, M. Presi, A. D'Errico, E. Ciaramella, *IEEE Photon. Technol. Lett.* **20**, 791 (2008)
12. L. Yi, Y. Jaouën, W. Hu, J. Zhou, Y. Su, E. Pincemin, *Opt. Lett.* **32**, 3182 (2007)
13. K. Voigt, L. Zimmermann, G. Winzer, T. Mitze, J. Bruns, K. Petermann, B. Hüttl, C. Schubert, *IEEE Photon. Technol. Lett.* **20**, 614 (2008)
14. L. Christen, Y. Lizé, S. Nuccio, A.E. Willner, L. Paraschis, *Opt. Express* **16**, 3828 (2008)
15. M.P. Fok, C. Shu, *Opt. Lett.* **33**, 2845 (2008)
16. C. Langrock, S. Kumar, J.E. McGeehan, A.E. Willner, M.M. Fejer, *J. Lightwave Technol.* **24**, 2579 (2006)
17. M.H. Chou, I. Brener, M.M. Fejer, E.E. Chaban, S.B. Christman, *IEEE Photon. Technol. Lett.* **11**, 653 (1999)
18. C.Q. Xu, B. Chen, *Opt. Lett.* **29**, 292 (2004)
19. B. Chen, C.Q. Xu, *IEEE J. Quantum Electron.* **40**, 256 (2004)
20. J. Wang, J. Sun, C. Luo, Q. Sun, *Opt. Express* **13**, 7405 (2005)
21. J. Yamawaku, H. Takara, T. Ohara, A. Takada, T. Morioka, O. Tadanaga, H. Miyazawa, M. Asobe, *IEEE J. Sel. Top. Quantum Electron.* **12**, 521 (2006)
22. H. Furukawa, A. Nirmalathas, N. Wada, S. Shinada, H. Tsuboya, T. Miyazaki, *IEEE Photon. Technol. Lett.* **19**, 384 (2007)
23. P. Martelli, P. Boffi, M. Ferrario, L. Marazzi, P. Parolari, R. Siano, V. Pusino, P. Minzioni, I. Cristiani, C. Langrock, M.M. Fejer, M. Martinelli, V. Degiorgio, *Opt. Express* **17**, 17758 (2009)
24. Y. Wang, C. Yu, L. Yan, A.E. Willner, R. Roussev, C. Langrock, M.M. Fejer, J.E. Sharping, A.L. Gaeta, *IEEE Photon. Technol. Lett.* **19**, 861 (2007)
25. I. Fazal, O. Yilmaz, S. Nuccio, B. Zhang, A.E. Willner, C. Langrock, M.M. Fejer, *Opt. Express* **15**, 10492 (2007)
26. L. Christen, O.F. Yilmaz, S. Nuccio, X. Wu, I. Fazal, A.E. Willner, C. Langrock, M.M. Fejer, *Opt. Lett.* **34**, 542 (2009)
27. H. Ishizuki, T. Suhara, M. Fujimura, H. Nishihara, *Opt. Quantum Electron.* **33**, 953 (2001)
28. D. Gurkan, S. Kumar, A.E. Willner, K.R. Parameswaran, M.M. Fejer, *J. Lightwave Technol.* **21**, 2739 (2003)

29. J. Wang, J. Sun, Q. Sun, Opt. Express **15**, 1690 (2007)
30. Y.L. Lee, B.-A. Yu, T.J. Eom, W. Shin, C. Jung, Y.-C. Noh, J. Lee, D.-K. Ko, K. Oh, Opt. Express **14**, 2776 (2006)
31. S. Kumar, A.E. Willner, D. Gurkan, K.R. Parameswaran, M.M. Fejer, Opt. Express **14**, 10255 (2006)
32. J.E. McGeehan, M. Giltrelli, A.E. Willner, Electron. Lett. **43**, 409 (2007)
33. J.E. McGeehan, S. Kumar, A.E. Willner, Opt. Express **15**, 5543 (2007)
34. J. Wang, J.Q. Sun, Q.Z. Sun, D.L. Wang, M.J. Zhou, X.L. Zhang, D.X. Huang, M.M. Fejer, Appl. Phys. Lett. **91**, 051107 (2007)
35. S.L. Jansen, D. van den Borne, P.M. Krummrich, S. Spälter, G.D. Khoe, H. de Waardt, IEEE J. Sel. Top. Quantum Electron. **12**, 505 (2006)
36. J. Wang, J. Sun, X. Zhang, D. Huang, M.M. Fejer, Opt. Lett. **33**, 1804 (2008)